Topics in Catalysis (2019) 62:639–648
https://doi.org/10.1007/s11244-019-01146-5

ORIGINAL PAPER

Oxidative Depolymerisation of Lignosulphonate Lignin into Low-Molecular-Weight Products with Cu–Mn/δ-Al_2O_3

Omar Y. Abdelaziz[1,2] · Sebastian Meier[3] · Jens Prothmann[4] · Charlotta Turner[4] · Anders Riisager[2] · Christian P. Hulteberg[1]

Published online: 5 March 2019

Abstract

Lignin depolymerisation receives great attention due to the pressing need to find sustainable alternatives to fossil sources for production of fuels and chemicals. In this study, alumina-supported Cu–Mn and Ni–Mo catalysts were tested for oxidative depolymerisation of a technical lignin stream—sodium lignosulphonates—to produce valuable low-molecular-weight aromatics that may be considered for applications in the fuels and chemicals sector. The reactions were performed at elevated temperature and oxygen pressure, and the product mixtures were analysed by size exclusion chromatography, two-dimensional nuclear magnetic resonance spectroscopy and supercritical fluid chromatography mass spectrometry. The best performance was obtained with Cu–Mn/δ-Al_2O_3, which was thoroughly characterised before and after use by nitrogen physisorption, scanning electron microscopy, energy dispersive spectroscopy, powder X-ray diffraction, thermal gravimetric analysis, inductively coupled plasma optical emission spectrometry and X-ray photoelectron spectroscopy. Major products identified were vanillin, *p*-hydroxybenzaldehyde, vanillic acid and *p*-hydroxybenzoic acid as well as smaller aliphatic aldehydes, acids and lactones.

Keywords Catalytic oxidation · Cu–Mn/Al_2O_3 catalyst · Heterogeneous catalysis · Lignin valorisation · Sodium lignosulphonates

1 Introduction

Utilisation of renewable raw materials as a source of energy, chemicals and materials is expected to increase in the near future. This supports emerging biorefinery strategies and new circular bioeconomy concepts moving towards better valorisation of lignocellulosic biomass. Lignin is one of the main constituents (polymeric wood components) of terrestrial plant biomass, together with the carbohydrate polymers cellulose and hemicellulose. It is a complex biopolymer consisting of phenylpropanoid subunits and accounts for approximately 15–30% of the woody biomass dry weight, providing structural integrity to the terrestrial lignocellulosic material [1–3]. Lignin is recognised as the third most abundant biopolymer available on Earth after cellulose and chitin, providing a potential source for production of renewable materials and high-value products [3, 4]. Large amounts of this heterogeneous substrate are already generated each year as a low-value by-product of the pulp and paper industry; transforming it into homogeneous and usable fractions with higher value is of great importance.

Electronic supplementary material The online version of this article (https://doi.org/10.1007/s11244-019-01146-5) contains supplementary material, which is available to authorized users.

✉ Omar Y. Abdelaziz
omar.abdelaziz@chemeng.lth.se

✉ Anders Riisager
ar@kemi.dtu.dk

✉ Christian P. Hulteberg
christian.hulteberg@chemeng.lth.se

[1] Department of Chemical Engineering, Lund University, P.O. Box 124, 221 00 Lund, Sweden

[2] Centre for Catalysis and Sustainable Chemistry, Department of Chemistry, Technical University of Denmark, 2800 Kgs. Lyngby, Denmark

[3] Department of Chemistry, Technical University of Denmark, 2800 Kgs. Lyngby, Denmark

[4] Centre for Analysis and Synthesis, Department of Chemistry, Lund University, P.O. Box 124, 221 00 Lund, Sweden

Despite its potential, lignin remains a greatly underutilised biopolymer in contrast to other lignocellulosic polymeric components [5], and its efficient valorisation presents an ongoing challenge. It is most commonly used as a low-cost fuel for heat and power generation, since it has the highest specific energy content available in the organic matrix of lignocellulosic materials due to its more reduced carbons [6]. In contrast, only a minor portion is being commercialised and transformed to other valuable products and applications.

The challenges in using lignin as a raw material for low-molecular-weight (LMW) chemicals production [7] result from the fact that the polymer is markedly heterogeneous, hindering the disassembling of its phenolic building blocks. Technical (industrial) lignins are particularly challenging compared to other native lignin streams. A principal reason is that such streams contain primarily C–C inter-unit bonds having high bond dissociation energy [8, 9], unlike C–O ether bonds, which are more easy to cleave.

Sulphur-containing lignin streams are generated in large scale on-site pulp mills, such as in sulphate (Kraft) and sulphite pulping. Lignin from sulphite processes is denoted as lignosulphonates, and is produced by means of sulphurous acid and/or a sulphite salt containing ammonium, magnesium, calcium, or sodium at different pH levels [10]. Lignosulphonates are less pure, have a higher molecular weight and contain higher sulphur contents than Kraft lignin. However, lignosulphonates have a unique property that makes them different from other available lignin streams: they are water-soluble. Due to the presence of sulphonated groups, lignosulphonates are negatively charged and water-soluble at neutral pH. A fragment representing the structure of sodium lignosulphonate lignin (used in this study) is schematically shown in Fig. 1.

Various lignin depolymerisation and conversion methods have been described in the literature, each approach having its own advantages and limitations. Examples comprise acid-catalysed [11, 12], base-catalysed [13, 14], thermochemical [15, 16], biochemical [1, 17], reductive [18, 19] and oxidative [20–22] lignin depolymerisation. Oxidative depolymerisation, in particular, emerges as a promising route among the deconstruction strategies, as it can produce highly functionalised chemicals under relatively mild operating conditions. Numerous efforts concerning oxidative depolymerisation of lignin model compounds have been reported, while only a few have considered real lignin substrates (raw lignin) as an option to investigate new functionalities and structures of the formed monomers, oligomers and organic acids [23, 24]. Heterogeneous catalysts may offer a number of advantages for oxidative depolymerisation of lignin, not only in terms of easy separation and recyclability, but also when the reactions are performed in the presence of molecular O_2 or other viable oxidants.

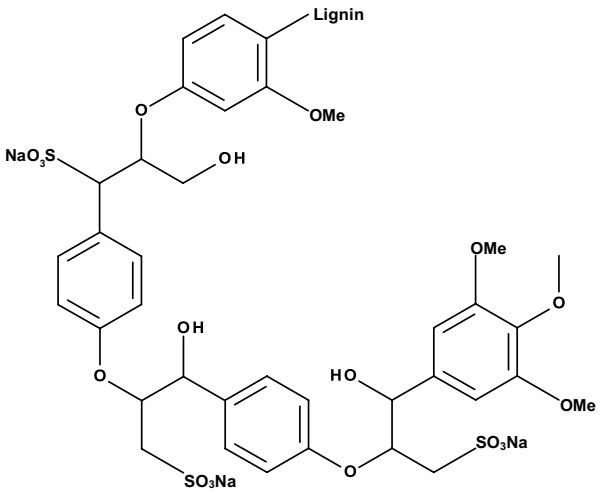

Fig. 1 Representative chemical structure of sodium lignosulphonate lignin

In the present study, different heterogeneous catalysts were tested for their ability to depolymerise sodium lignosulphonates—a technical lignin stream—into LMW aromatics using molecular O_2 without additional solvent. The catalyst performance was evaluated using various characterisation techniques, and the product mixtures were thoroughly analysed to elucidate structural features.

2 Experimental

2.1 Chemicals and Materials

Sodium lignosulphonate lignin (LS) was kindly provided by Domsjö Fabriker AB (Örnsköldsvik, Sweden) and used as starting raw material. Proximate and ultimate analyses as well as the high heating value of LS substrate are reported in Table 1. Oxygen gas (≥ 99.5%) was obtained from AGA, Denmark, methanol and ethyl acetate (LC–MS grades) purchased from Merck, Germany, and ammonia (2 M in methanol) purchased from Fisher Scientific, USA. Unless otherwise mentioned, all other chemicals and reagents were purchased from Sigma-Aldrich or VWR and used as received without further purification.

2.2 Catalyst Preparation

The catalysts used were all based on an extruded δ-Al_2O_3 support crushed to 20–30 mesh (1–2 mm). Cu–Mn/δ-Al_2O_3 (Cat A) was prepared by incipient wetness impregnation (IWI) of a mixture of the Cu and Mn acetate salts, repeated twice. The samples were dried and calcined at 350 °C for 1 h after each impregnation, resulting in a catalyst composition

Table 1 Elementary analysis and higher heating value of lignosulphonate lignin. The values are reported on a dry basis, with available uncertainty (95% confidence interval). The oxygen content was calculated by difference

Analysis	Lignosulphonate lignin (LS)
Proximate analysis	
Ash (%)	26.9
Volatiles (%)	60.3
Fixed carbon (%)	12.8
Moisture (%)	3.3
HHV (MJ kg^{-1})	16
Ultimate analysis (% dry basis)	
C	42.9
H	4.4
N	0.8
S	7.9
O	17.1

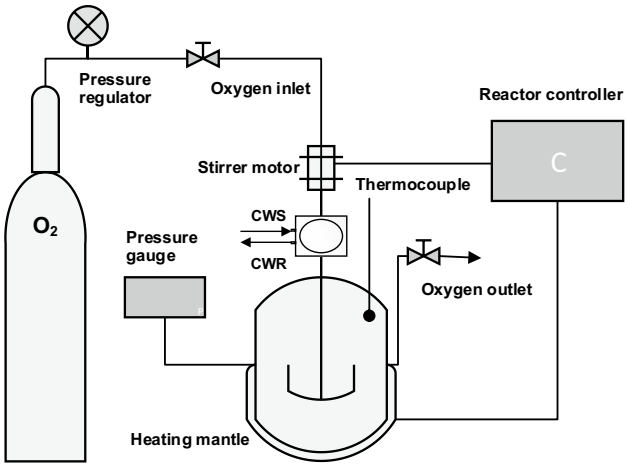

Fig. 2 Schematic illustration of setup used for lignin oxidative depolymerisation experiments

of 3% Cu and 6% Mn. Ni–Mo/δ-Al_2O_3 (Cat B) was also prepared by IWI using the nitrate salts of Ni and Mo, starting with Mo impregnation, calcination at 500 °C for 2 h and then Ni impregnation, followed by calcination at 500 °C for 2 h, resulting in a catalyst composition of 3% Ni and 6% Mo. Sulphided Ni–Mo/δ-Al_2O_3 (Cat C) was prepared by treating Cat B with 100 ppm H_2S in N_2 for 16 h (GHSV 400 h^{-1}) using a temperature ramp from 25 to 400 °C followed by a hold time of 10 h. After sulphidation, the catalyst was waxed using a C_{18} saturated hydrocarbon (octadecane) to ensure the sulphidated catalyst remain intact.

2.3 Catalytic Oxidation Reactions

The oxidative depolymerisation experiments were carried out in a 100 mL mechanically stirred Parr reactor equipped with a 4843 PID temperature controller (Parr Instruments Company, Moline, Illinois, USA). Three heterogeneous catalysts and the support were screened and tested for their ability to depolymerise the LS substrate under O_2 pressure. A schematic diagram of the experimental setup used in this study is shown in Fig. 2.

Typically, in a single run, the reactor was loaded with 30 mL of deionised water (DI), 600 mg of LS substrate and 300 mg of catalyst (catalyst-to-lignin ratio = 1:2 w/w). The reactor was purged (at least twice) and pressurised with molecular O_2 to 15 bar, where after the reactor under stirring (400 rpm) was heated to the reaction temperature of 160 °C. The reaction time was counted from the onset of the set temperature (heating time ~ 40 min). After completion of the reaction, the reactor was directly quenched in an ice bath and depressurised at room temperature (cooling time ~ 5 min).

2.4 Analysis of Products

The product mixtures were analysed using size exclusion chromatography (SEC), 2D nuclear magnetic resonance (NMR) spectroscopy and supercritical fluid chromatography mass spectrometry (SFC-MS).

2.4.1 SEC Analysis

The molecular weight distribution (MWD) and sizes of LS substrate and produced reaction mixtures were determined using a SEC system, as described in our previously developed method for technical lignin samples [25]. In brief, the system was a Waters 600E high-performance liquid chromatography setup (Waters, Milford, MA, USA) fitted with a Waters 2414 refractive index detector, a Waters 486 ultraviolet (UV) absorbance detector and an analytical column packed with 60 cm of Superdex 30 and 200 prep grade (GE Healthcare, Uppsala, Sweden). The column was operated at room temperature and eluted with 125 mM NaOH solution at a flowrate of 1.0 mL/min. Calibration was done using polyethylene glycol (PEG) standards ranging from 0.4 to 35 kDa (Merck Schuchardt OHG, Hohenbrunn, Germany). The samples were diluted at concentrations of 0.5 g/L in the eluent and the solutions were filtered using a 0.2 µm filter (Schleicher and Schuell, Dassel, Germany) to remove any suspended matter. The filtered solution (500 µL) was injected into the SEC system for data acquisition. Due to comparison with PEG standards, the molecular weight and the molecular number should be interpreted relatively.

2.4.2 NMR Spectroscopy

NMR samples of LS substrate and reaction products were prepared by mixing 500 µL substrate or product solution with 50 µL D_2O (Sigma-Aldrich, 99.9% D) in 5 mm NMR sample tubes. For product identification, ^1H–^{13}C HSQC and ^1H–^1H TOCSY spectra were acquired for product mixtures and for authentic reference compounds of acetaldehyde, formaldehyde, methanol, acetic acid, β-hydroxy-γ-butyrolactone, α-hydroxy-γ-butyrolactone, succinic acid, malic acid and maleic acid at 25 °C on a Bruker Avance III 800 MHz spectrometer equipped with a TCI CryoProbe. The ^1H–^{13}C HSQC spectra had a carrier offset of 75 ppm and a spectral width of 165 ppm in the ^{13}C dimension. ^1H–^{13}C HSQC spectra were recorded as data matrices of 2048 × 256 complex data points sampling the NMR signal for 159 and 7.7 ms in the ^1H and ^{13}C dimensions, respectively. A multiplicity-edited ^1H–^{13}C HSQC spectrum was acquired on the product mixture in order to gain additional structural insight by distinguishing CH, CH_2 and CH_3 groups. ^1H–^1H TOCSY spectra were acquired as data matrices of 1024 × 256 complex data points sampling the NMR signal for 128 and 32 ms in the direct and indirect ^1H dimension, respectively. The ^1H–^1H TOCSY spectra were acquired with a spectral width of 10 ppm in both dimensions around a carrier offset of 4.7 ppm using a 10 kHz spin lock field during a mixing time of 80 ms. A double quantum-filtered ^1H–^1H COSY spectrum of the water soluble product was acquired as a data matrix of 1024 × 256 complex data points with a spectral width of 13.3 ppm in both dimensions, sampling the NMR signal for 96 and 24 ms in the direct and indirect ^1H dimension, respectively. All spectra were processed with a shifted sine-bell apodisation function and extensive zero filling in both dimensions in Topspin 3.5.

2.4.3 SFC-MS Analysis

The LS substrate and reaction products were analysed using SFC-MS to reveal monomeric compounds present. Prior to analysis, the sample preparation was performed as described in our previously published method for the analysis of lignin monomers [26]; 10 mL of LS sample and the reaction product were acidified to pH 1 using 6 M HCl, and precipitates removed by centrifugation. The supernatants were extracted with 10 mL ethyl acetate (2 × 3 mL + 1 × 4 mL), and the corresponding extracts combined and the ethyl acetate evaporated under a nitrogen stream. The solid residues were redissolved in 3 mL ethyl acetate and filtered with a 0.2 µm polytetrafluoroethylene membrane syringe filter.

A Waters Ultra Performance Convergence Chromatography System (Waters, Milford, MA, USA) equipped with a Waters Torus DIOL (1.7 µm, 3 mm × 100 mm) and a Waters Torus Van-Guard pre-column (1.7 µm, 2.1 mm × 5 mm) was connected via a flow splitter (ACQUITY UPC^2 splitter, Waters) to a Waters XEVO-G2 QTOF-MS (Waters). A modified method of our previously published approach for the identification of lignin monomers using ultra-high-performance supercritical fluid chromatography/high resolution mass spectrometry (UHPSFC/HRMS) was used for analysis [26]. In short, a DIOL column was used with a column temperature of 50 °C, a flow rate of 2 mL and a backpressure of 130 bar. For the elution, a gradient was used starting with 0% B (vol%) and then ramped to 8.5% (vol%) until 2.5 min. Then B was increased to 25% (vol%) until 5.5 min and then held for 2 min. Then B was reduced in 0.5 min to 0% (vol%) and the column was equilibrated for 2 min with the starting condition before the next injection. The solvents were CO_2 (A) and methanol (B) and the injection volume was 1.5 µL. As a makeup solvent, methanol with 5 mM ammonia was used with a flow rate of 0.4 mL/min. The electrospray ionisation source was used in negative mode with a source temperature of 120 °C, a desolvation gas temperature of 600 °C, a desolvation gas flow of 1200 L/h, a cone voltage of 20 V and a capillary voltage of 3 kV. Both samples were analysed in full scan mode and in MS^2 mode. For the MS^2 mode, a collision induced dissociation energy ramp from 10 to 35 V was used.

2.5 Characterisation of Catalysts

The fresh and spent samples of best performing catalyst were characterised with Brunauer–Emmett–Teller (BET) nitrogen adsorption–desorption, scanning electron microscopy (SEM), energy dispersive spectroscopy (EDS) elemental mapping, powder X-ray diffraction (XRD), thermal gravimetric analysis (TGA), inductively coupled plasma optical emission spectrometry (ICP-OES) and X-ray photoelectron spectroscopy (XPS).

N_2 nitrogen physisorption measurements were performed at − 196 °C using an ASAP 2020 Micromeritics instrument (Norcross, GA, USA) for examining surface areas and porous structures of the catalyst samples. The samples were degassed at 200 °C under vacuum for 4 h prior to measurements, and the specific surface areas were estimated according to the BET method.

The morphology of the catalyst samples was examined through a high-resolution SEM (FEI Quanta 200F), fitted with an Everhart–Thornley detector (ETD). The images were recorded at low accelerating voltage (2 kV), with a spot size of 3, and with 1000 times magnification. EDS was used in connection with SEM for the elemental mapping and map sum spectra acquisition. The elemental mapping was collected using the same spectrophotometer.

Powder XRD analysis was performed with a Huber G670 diffractometer using Cu$K_{\alpha 1}$ radiation (λ = 1.54 Å) within a

2θ range of 3–100°, emitting from a focusing quartz monochromator. The radiation exposure time was 60 min.

TGA was carried out in a dynamic air environment using a Mettler Toledo Star^e thermal analyser (model TGA/DSC 1) in the temperature interval 25–600 °C with a constant heating rate of 10 °C/min. The thermal program was paused at 600 °C for 1 h during measurement.

The samples used for ICP-OES analysis (500 mg of catalyst per analysis) were dissolved in 7 mL of HNO_3 and 3 mL of water in a Mar5 microwave oven in a closed Teflon vessel, in which both temperature and pressure were controlled. The samples were then diluted 5 times with deionised water before analysis using an Optima 8300 from PerkinElmer (Waltham, MA, USA).

XPS spectra were acquired with a Thermo Scientific system at room temperature using monochromated AlK_α radiation (1484.6 eV). The base pressure in the analysis chamber was maintained at 2×10^{-7} mbar. The numbers of scans were 20, 20, 10 and 4 for Mn, Cu, Al and O, respectively.

3 Results and Discussion

3.1 Molecular Weight and Structural Features

To examine the variations between the lignin substrate and produced reaction products, the samples were analysed and compared in terms of molecular weight distribution and chemical structure. Figure 3 depicts the SEC curves of the initial LS substrate and the product mixtures generated from different experimental runs.

As can be seen, the Cu–Mn/δ-Al_2O_3 catalyst showed superior performance for converting the high-molecular-weight LS material into LMW products (M_p ~ 1.4 kDa).

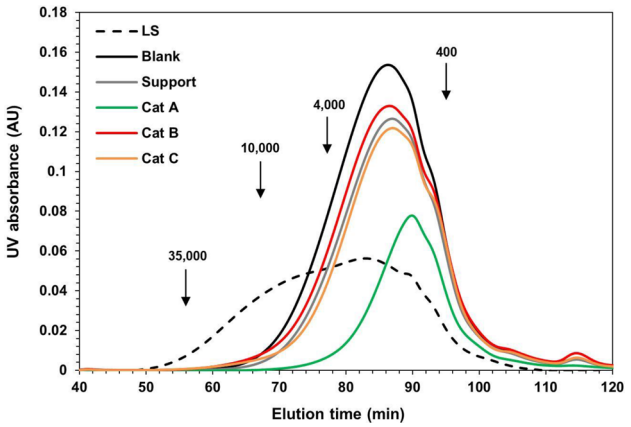

Fig. 3 Size exclusion chromatograms of lignosulphonate lignin and depolymerised samples with characteristic UV absorption at 280 nm. The arrows point to the molecular weight (Da) of the PEG standards that were used for calibration

In comparison to other investigated catalysts, the higher catalytic performance of Cu–Mn/δ-Al_2O_3 can be explained by the ability of transition metal ions – Mn and Cu – to form highly oxidised metallo–oxo complexes upon reaction with the molecular O_2. The product fractions also exhibited much narrower molecular weight distributions in comparison to the starting material, which exhibited a rather broad peak constituting exceedingly heavy molecules. The product fraction generated over Cu–Mn/δ-Al_2O_3, on the other hand, showed a maximum range of 10 kDa for heaviest contained molecules, suggesting that an effective depolymerisation process was achieved. The products generated over alumina support, Ni–Mo/δ-Al_2O_3 and sulphided Ni–Mo/δ-Al_2O_3 showed slightly better performance (molecular weight reductions) than the blank experiment. However, the changes were not significant, and Cu–Mn/δ-Al_2O_3 was thus selected for further detailed analysis.

In addition, it was revealed from the NMR measurements that there were notable differences in the chemical compositions of the LS sample and the product sample generated utilising Cu–Mn/δ-Al_2O_3 catalyst, particularly in the inter-unit/oxygenated aliphatic region. Figure 4 compares 2D ^{1}H–^{13}C HSQC spectra acquired in water of the original LS lignin (Fig. 4a) and of the product mixture obtained upon oxidative depolymerisation using Cu–Mn/δ-Al_2O_3 catalyst (Fig. 4b; see supplementary material Fig. S1 for a full overlay of substrate and product spectra). The spectra validate that LS is rich in guaiacyl content and low in syringyl content, with some residual xylan likely present from original pretreatment. Spectral comparison shows that oxidative depolymerisation vastly abolishes methoxy group signals (δ^1H ~ 3.5–4 ppm, δ^{13}C ~ 55 ppm) as well as other signals in the side-chain interunit linkage region (aliphatic oxygenated groups at δ^{13}C ~ 60–90 ppm). As C–C linkages constitute a considerable fraction of the interunit linkages present in technical lignin, the findings here suggest that Cu–Mn/δ-Al_2O_3 catalyst is capable of catalysing C–C bond cleavage of the propyl side-chain in the LS lignin structural units.

Consistent with recent reports for a chelator-mediated Fenton reaction [27], the water-soluble post-reaction material is also largely devoid of aromatic ^{1}H–^{13}C HSQC signals in our depolymerisation system. A variety of product signals can be observed. These products were characterised by the use of authentic reference standards and homonuclear assignment spectra (^{1}H–^{1}H TOCSY spectra) as well as multiplicity-edited ^{1}H–^{13}C HSQC to identify spin systems and structural motifs in the product molecules. Figure 4b shows an assigned ^{1}H–^{13}C HSQC spectrum with some molecules in the product mixture highlighted. Consistent with the loss of methoxy signal, the product mixture included methanol and its oxidation products formaldehyde (detected as the hydrate form) and formic acid as well as acetaldehyde (detected as hydrate and free aldehyde form) and acetic acid.

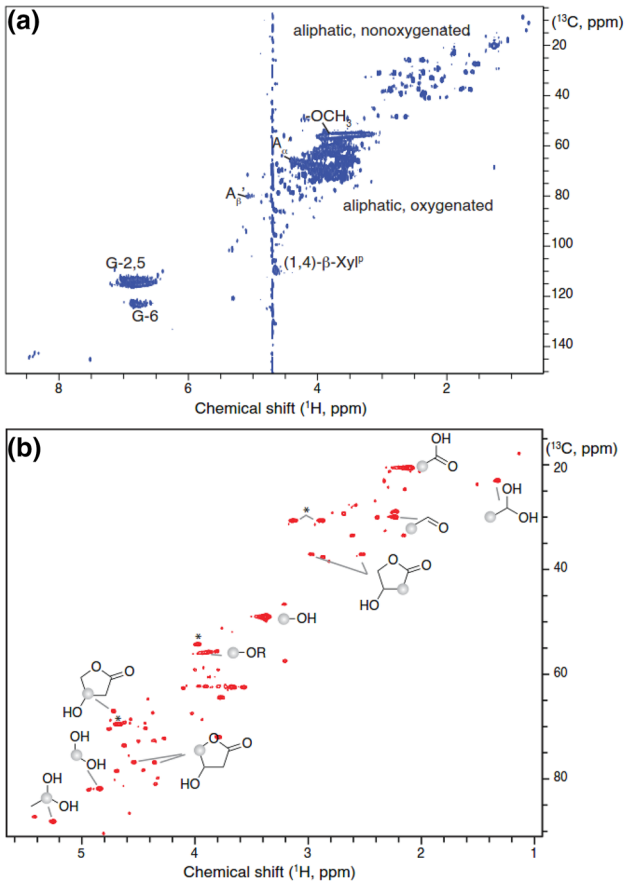

Fig. 4 Two-dimensional $^{1}H–^{13}C$ HSQC NMR spectrum of lignosulphonate lignin substrate (**a**) and spectrum of identified reaction products in oxidatively depolymerised sample using Cu–Mn/δ-Al_2O_3 catalyst, with the sphere indicating the CH group corresponding to indicated spectral signals (**b**). Products include methanol, formaldehyde, formic acid, acetaldehyde, acetic acid and β-hydroxy-γ-butyrolactone. The asterisk indicates a major mixture component that is tentatively assigned to the β-sulphonate derivative of γ-butyrolactone

The presence of these aldehydes in the product mixture indicates a stepwise reaction with aldehydes formed as highly populated intermediates. Notably, the product mixture also included larger polyhydroxylated carbonyl containing compounds such as β-hydroxy-γ-butyrolactone in addition to the β-sulphonate derivative of γ-butyrolactone (Fig. 4b). In a recent study, lactone species were identified as key condensation product in technical lignin streams [28], consistent with the presence of novel lactone markers. Unlike β-hydroxy-γ-butyrolactone, α-hydroxy-γ-butyrolactone was not observed in significant amount in the product mixture.

SFC-MS analysis was done to achieve qualitative molecular information about the samples. The base peak ion chromatograms of the LS and the oxidatively depolymerised lignosulphonate after reaction with Cu–Mn/δ-Al_2O_3 (Cat A) are shown in Fig. 5.

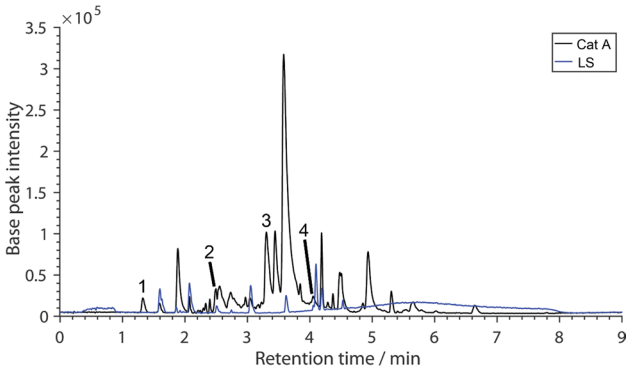

Fig. 5 Base peak ion chromatograms obtained from the SFC-MS analysis for lignosulphonate lignin (LS) substrate and oxidatively depolymerised product using Cu–Mn/δ-Al_2O_3 catalyst (Cat A). Peak identities: vanillin (1), *p*-hydroxybenzaldehyde (2), vanillic acid (3) and *p*-hydroxybenzoic acid (4)

Comparing the chromatograms, it can be seen that the catalytically treated sample showed more monomers than the LS sample and only vanillic acid was identified in the latter based on the retention time, exact mass and observed fragments (Table S1). In contrast, the four lignin monomers vanillin, *p*-hydroxybenzaldehyde, vanillic acid and *p*-hydroxybenzoic acid were identified by the same identification criteria in the catalytically depolymerised sample (Table S1). Vanillic acid was identified in both samples, but the significant difference in the peak intensities in the extracted ion chromatograms (Figs. S2 and S11) showed that additional vanillic acid was produced during the course of the oxidation reaction. The extracted ion chromatograms, mass spectra and MS^2 spectra for all identified compounds are shown in Figs. S2 to S16 (supplementary material).

3.2 Catalyst Characterisation

The δ-Al_2O_3 support used for the experiments had a specific surface area as measured by nitrogen physisorption of 128 m^2/g and a pore volume of 0.54 cm^3/g. The calculated average pore size (assuming cylindrical pores) was 16.7 nm. The rather open pore system was quite well in line with the sizes of lignin macromolecules reported, which are in the 1–40 nm range depending on source and extraction method [29], indicating that all catalyst inventory was available for reaction. Adding the active phase to the support slightly lowered the measured surface area (118 m^2/g for the Cu/Mn-catalyst and 116 m^2/g for the Ni/Mo-catalyst). The spent catalysts showed higher surface area than the fresh ones, probably due to carbon deposits in the catalyst pores. Due to the wax used in conserving the sulphided Ni–Mo catalyst, it was not possible to perform accurate BET analysis for Cat C. All properties as derived from the nitrogen physisorption measurements are summarised in Table 2.

Table 2 Textural properties as calculated by BET analysis

Catalyst	Specific surface area ($m^2\ g^{-1}$)	Pore size (nm)	Pore volume ($cm^3\ g^{-1}$)
δ-Al_2O_3 fresh	128.4	16.7	0.54
δ-Al_2O_3 spent	129.8	14.4	0.47
Cu–Mn/δ-Al_2O_3 fresh	118.1	15.6	0.46
Cu–Mn/δ-Al_2O_3 spent	145.3	11.8	0.43
Ni–Mo/δ-Al_2O_3 fresh	115.7	13.7	0.40
Ni–Mo/δ-Al_2O_3 spent	141.8	12.8	0.45

SEM images were obtained for the δ-Al_2O_3 catalyst support (Fig. 6a), the fresh Cu–Mn/δ-Al_2O_3 (Fig. 6b) and the spent Cu–Mn/δ-Al_2O_3 (Fig. 6c) to visualise the morphology of the materials. The images of the alumina support and the fresh catalyst showed only minor differences between the materials before and after the addition of the active phase on the 100 µm scale, whereas significant differences were found between the two fresh samples and the spent catalyst. Thus, in the spent catalyst, an uneven top-layer (dark grey areas) with islands of catalyst appeared to rise above the support surface.

TG analysis (Fig. 7) of the fresh and spent catalysts were quite different with the spent material losing much more weight between 300 and 450 °C – almost 10 wt% – compared to the fresh catalyst. This difference was attributed to vaporisation of heavier organic compounds, thermal decomposition of polymers and, at higher temperatures, oxidation of solid carbon, thus likely corresponding to the top-layer, which also induced a lowering of the BET surface area as discussed above.

SEM–EDS images with corresponding elemental spectra of the fresh and spent Cu–Mn/δ-Al_2O_3 catalyst, respectively (Fig. 8), further revealed a significant increase in the sulphur

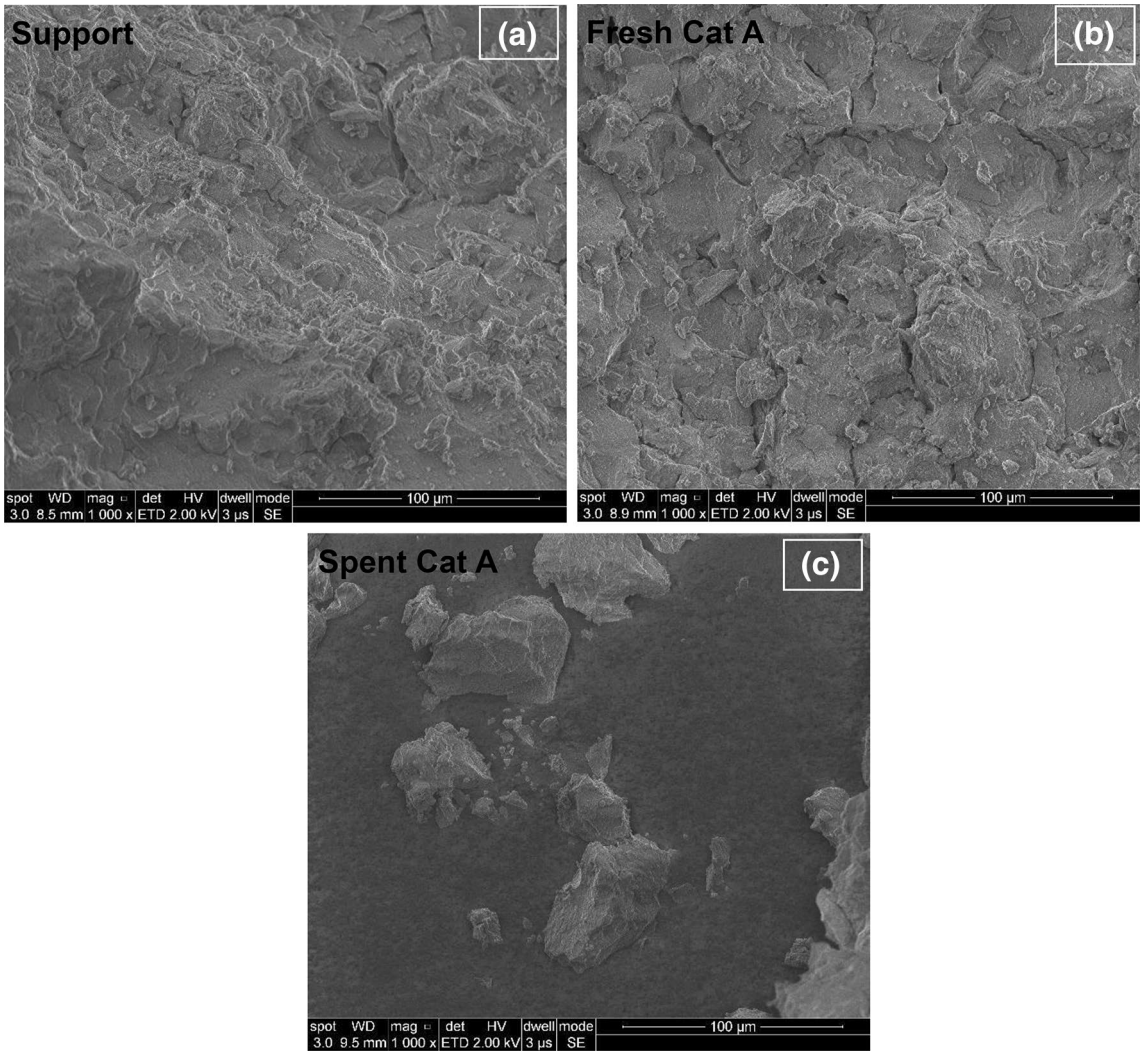

Fig. 6 SEM images of the **a** δ-Al_2O_3 support, **b** fresh Cu–Mn/δ-Al_2O_3 catalyst and **c** spent Cu–Mn/δ-Al_2O_3 catalyst

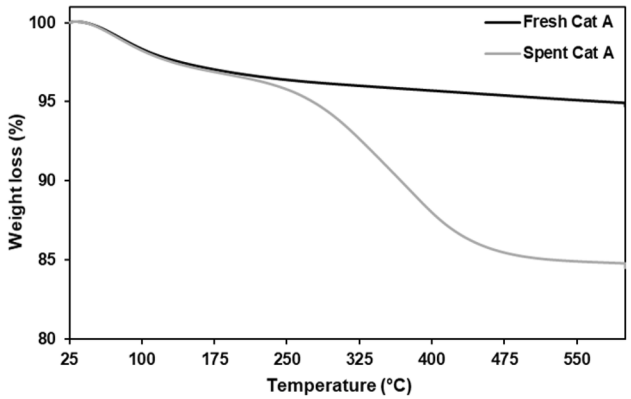

Fig. 7 TGA curves of the fresh and spent Cu–Mn/δ-Al_2O_3 catalyst

amount in the spent catalyst compared to the fresh catalyst. In addition, the signal intensity with respect to Mn and Cu appeared to be lower in the spent catalyst, which may be due to the previously mentioned top-layer. Notably, no changes in the bulk of the catalyst were indicated from the powder X-ray diffraction patterns of the materials (Fig. 9), which revealed only diffractions peaks consistent with δ-Al_2O_3 at 2θ of 32, 36, 45, 61, 67 and 85° [30].

The catalyst surface composition was further investigated using XPS and revealed several differences between the fresh and spent catalysts according to the analysis in Table 3. First, a high surface sulphur content of 1.7 atomic% was found for the spent catalyst after the lignin oxidative depolymerisation reaction. Second, the spent catalyst had a significantly lower surface concentration of Mn (0.4 atomic% against 3.3 atomic% in the fresh catalyst), whereas the surface Cu concentration remained almost unchanged. The decrease in Mn content clearly indicated leaching of Mn from the supported catalyst during operation, which may also have contributed to the observed catalytic activity as Mn ions have been reported to be active for lignin depolymerisation reactions [31].

The leaching of Mn was confirmed and quantified using ICP-OES analysis. The measured composition of the fresh

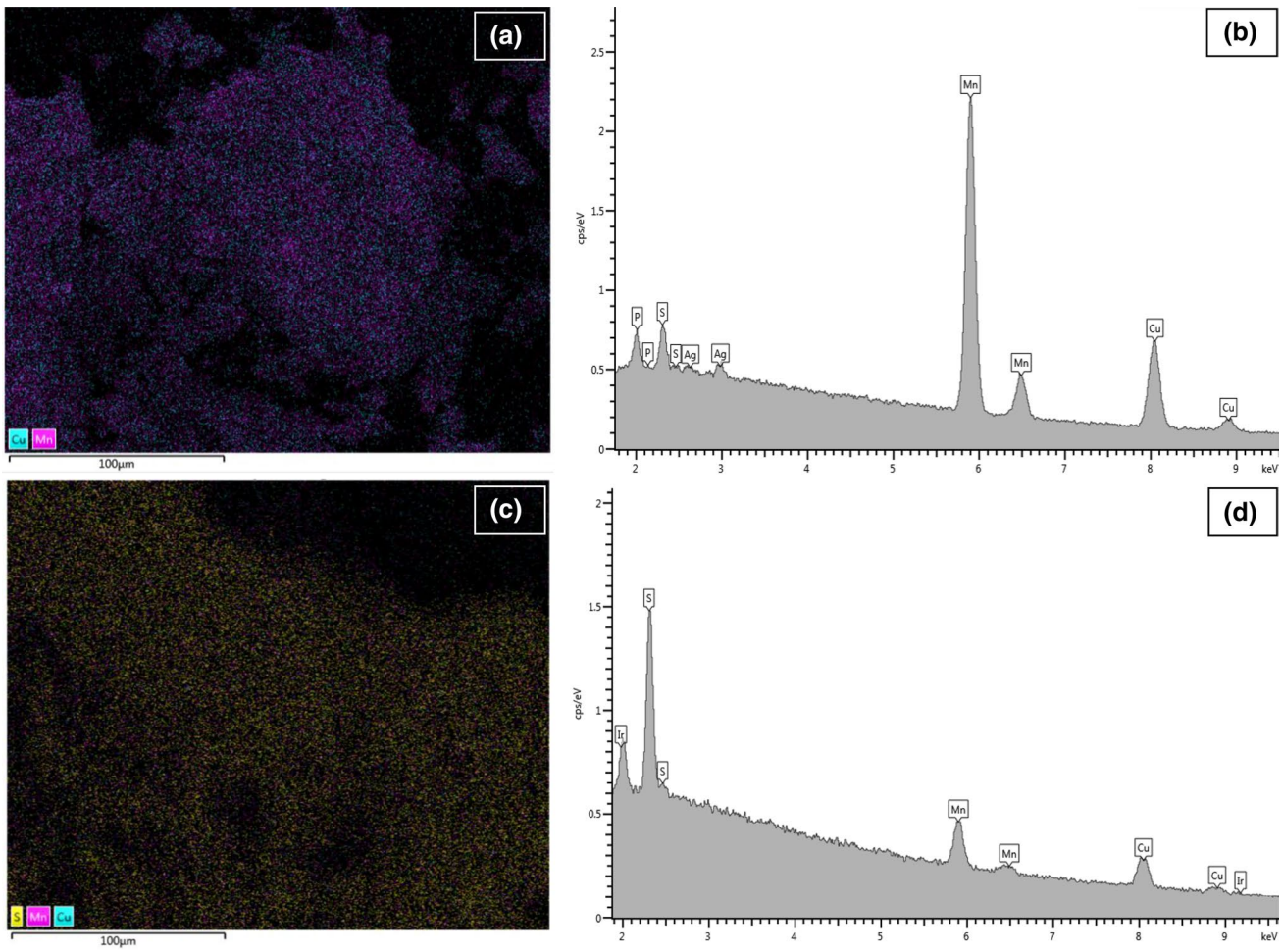

Fig. 8 SEM–EDS elemental mapping and map sum spectra of the **a, b** fresh Cu–Mn/δ-Al_2O_3 catalyst and **c, d** spent Cu–Mn/δ-Al_2O_3 catalyst

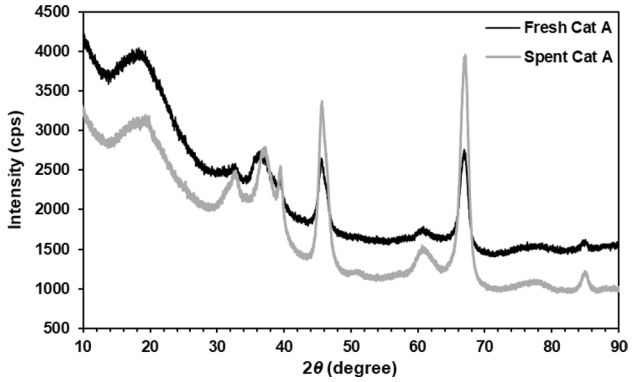

Fig. 9 XRD patterns of the fresh and spent Cu–Mn/δ-Al_2O_3 catalyst

Table 3 Surface elemental composition (% atomic concentration) as determined by XPS

Catalyst	Al2p	O1s	Cu2p	Mn2p	S2p
Cu–Mn/δ-Al_2O_3 fresh	38.1	58.3	0.3	3.3	–
Cu–Mn/δ-Al_2O_3 spent	38.3	59.2	0.4	0.4	1.7

Cu–Mn/δ-Al_2O_3 catalyst was 3.15 wt% Mn and 2.29 wt% Cu; the catalyst contained no or very low amounts of sulphur. After the oxidative depolymerisation, the metal content in the catalyst were lowered to 0.34 wt% Mn and 0.48 wt% Cu, revealing that also Cu had leached from the catalyst even though the surface concentration apparently remained unchanged as found by XPS. Moreover, the sulphur content had increased considerably to 0.42 wt%. Combined, these results showed that the catalyst was not stable under the operating conditions tested, hindering the performance of recyclability tests and the investigation of catalyst reusability. Further optimisation is required to ensure long-term, stable operation.

4 Conclusions

Alumina-supported Cu–Mn and Ni–Mo catalysts were tested for their ability to depolymerise sodium lignosulphonates, a technical lignin stream generated from sulphite pulping. Under O_2 pressure, Cu–Mn/δ-Al_2O_3 showed a surpassing performance in converting LS into LMW compounds. Major compounds identified were vanillin, *p*-hydroxybenzaldehyde, vanillic acid and *p*-hydroxybenzoic acid in addition to smaller aliphatic aldehydes, acids and lactones. Such product streams can potentially be utilised in a diverse form of value-added applications in current fast-growing chemical and bio-based industries. Unfortunately, the long-term performance and the stability of the most active Cu–Mn/δ-Al_2O_3 catalyst was influenced negatively by the operating conditions, resulting in deposits of carbon- and sulphur-containing compounds on the catalyst surface as well as leaching of Mn and Cu ions. Hence, optimisation of catalyst durability remains a key for future work and possible successful industrial operation.

Acknowledgements This work was financed by the Swedish Foundation for Strategic Research (SSF) through grant contract RBP14-0052. O.Y. Abdelaziz acknowledges the internal funding of Lund University and Technical University of Denmark. Thanks to Hulteberg Chemistry & Engineering AB for providing the catalysts used in this study, and Gunnar Lidén for supplying the sodium lignosulphonates from Domsjö Fabriker AB. Bodil Fliis Holten, Sofia Mebrahtu Wisén, Leonhard Schill, Lise-Lotte Jespersen and Berit Wenzell are acknowledged for technical support with characterisation of the catalysts. 800 MHz NMR spectra were recorded by using the spectrometer of the NMR centre DTU supported by the Villum Foundation.

References

1. Gall DL, Ralph J, Donohue TJ, Noguera DR (2017) Biochemical transformation of lignin for deriving valued commodities from lignocellulose. Curr Opin Biotechnol 45:120–126. https://doi.org/10.1016/j.copbio.2017.02.015
2. Sjöström E (1993) Wood chemistry: fundamentals and applications, 2nd edn. Academic Press, San Diego
3. Calvo-Flores FG, Dobado JA, Isac-García J, Martín-Martínez FJ (2015) Lignin and lignans as renewable raw materials: chemistry, technology and applications. Wiley, Chichester
4. Bruijnincx PCA, Rinaldi R, Weckhuysen BM (2015) Unlocking the potential of a sleeping giant: lignins as sustainable raw materials for renewable fuels, chemicals and materials. Green Chem 17:4860–4861. https://doi.org/10.1039/c5gc90055g
5. Ragauskas AJ, Beckham GT, Biddy MJ et al (2014) Lignin valorization: improving lignin processing in the biorefinery. Science 344:1246843
6. Azadi P, Inderwildi OR, Farnood R, King DA (2013) Liquid fuels, hydrogen and chemicals from lignin: a critical review. Renew Sustain Energy Rev 21:506–523. https://doi.org/10.1016/j.rser.2012.12.022
7. Abdelaziz OY, Brink DP, Prothmann J et al (2016) Biological valorization of low molecular weight lignin. Biotechnol Adv 34:1318–1346. https://doi.org/10.1016/j.biotechadv.2016.10.001
8. Rinaldi R, Jastrzebski R, Clough MT et al (2016) Paving the way for lignin valorisation: recent advances in bioengineering, biorefining and catalysis. Angew Chemie Int Ed 55:8164–8215. https://doi.org/10.1002/anie.201510351
9. Guadix-Montero S, Sankar M (2018) Review on catalytic cleavage of C–C inter-unit linkages in lignin model compounds: towards lignin depolymerisation. Top Catal 61:183–198. https://doi.org/10.1007/s11244-018-0909-2
10. Aro T, Fatehi P (2017) Production and application of lignosulfonates and sulfonated lignin. ChemSusChem 10:1861–1877. https://doi.org/10.1002/cssc.201700082

11. Güvenatam B, Heeres EHJ, Pidko EA, Hensen EJM (2016) Lewis-acid catalyzed depolymerization of protobind lignin in supercritical water and ethanol. Catal Today 259:460–466. https://doi.org/10.1016/j.cattod.2015.03.041
12. Lahive CW, Deuss PJ, Lancefield CS et al (2016) Advanced model compounds for understanding acid-catalyzed lignin depolymerization: identification of renewable aromatics and a lignin-derived solvent. J Am Chem Soc 138:8900–8911. https://doi.org/10.1021/jacs.6b04144
13. Chaudhary R, Dhepe PL (2017) Solid base catalyzed depolymerization of lignin into low molecular weight products. Green Chem 19:778–788. https://doi.org/10.1039/C6GC02701F
14. Abdelaziz OY, Li K, Tunå P, Hulteberg CP (2018) Continuous catalytic depolymerisation and conversion of industrial kraft lignin into low-molecular-weight aromatics. Biomass Convers Biorefinery 8:455–470. https://doi.org/10.1007/s13399-017-0294-2
15. Pandey MP, Kim CS (2011) Lignin depolymerization and conversion: a review of thermochemical methods. Chem Eng Technol 34:29–41
16. Amen-Chen C, Pakdel H, Roy C (2001) Production of monomeric phenols by thermochemical conversion of biomass: a review. Bioresour Technol 79:277–299. https://doi.org/10.1016/S0960-8524(00)00180-2
17. Wu W, Dutta T, Varman AM et al (2017) Lignin valorization: two hybrid biochemical routes for the conversion of polymeric lignin into value-added chemicals. Sci Rep 7:8420. https://doi.org/10.1038/s41598-017-07895-1
18. Feghali E, Carrot G, Thuéry P et al (2015) Convergent reductive depolymerization of wood lignin to isolated phenol derivatives by metal-free catalytic hydrosilylation. Energy Environ Sci 8:2734–2743
19. Huang S, Mahmood N, Tymchyshyn M et al (2014) Reductive de-polymerization of kraft lignin for chemicals and fuels using formic acid as an in-situ hydrogen source. Bioresour Technol 171:95–102. https://doi.org/10.1016/j.biortech.2014.08.045
20. Rodrigues Pinto PC, Borges da Silva EA, Rodrigues AE (2011) Insights into oxidative conversion of lignin to high-added-value phenolic aldehydes. Ind Eng Chem Res 50:741–748. https://doi.org/10.1021/ie102132a
21. Ma R, Guo M, Zhang X (2018) Recent advances in oxidative valorization of lignin. Catal Today 302:50–60. https://doi.org/10.1039/9781788010351-00128
22. Tarabanko VE, Tarabanko N (2017) Catalytic oxidation of lignins into the aromatic aldehydes: general process trends and development prospects. Int J Mol Sci 18:2421. https://doi.org/10.3390/ijms18112421
23. Behling R, Valange S, Chatel G (2016) Heterogeneous catalytic oxidation for lignin valorization into valuable chemicals. What results? What limitations? What trends? Green Chem 18:1839–1854. https://doi.org/10.1039/c5gc03061g
24. Vangeel T, Schutyser W, Renders T, Sels BF (2018) Perspective on lignin oxidation: advances, challenges, and future directions. Top Curr Chem. https://doi.org/10.1007/s41061-018-0207-2
25. Abdelaziz OY, Hulteberg CP (2017) Physicochemical characterisation of technical lignins for their potential valorisation. Waste Biomass Valorization 8:859–869. https://doi.org/10.1007/s12649-016-9643-9
26. Prothmann J, Sun M, Spégel P et al (2017) Ultra-high-performance supercritical fluid chromatography with quadrupole-time-of-flight mass spectrometry (UHPSFC/QTOF-MS) for analysis of lignin-derived monomeric compounds in processed lignin samples. Anal Bioanal Chem 409:7049–7061. https://doi.org/10.1007/s00216-017-0663-5
27. Kent MS, Zeng J, Rader N et al (2018) Efficient conversion of lignin into a water-soluble polymer by a chelator-mediated Fenton reaction: optimization of H_2O_2 use and performance as a dispersant. Green Chem 20:3024–3037. https://doi.org/10.1039/c7gc03459h
28. Lancefield CS, Wienk HLJ, Boelens R et al (2018) Identification of a diagnostic structural motif reveals a new reaction intermediate and condensation pathway in kraft lignin formation. Chem Sci 9:6348–6360. https://doi.org/10.1039/c8sc02000k
29. Vainio U, Maximova N, Hortling B et al (2004) Morphology of dry lignins and size and shape of dissolved kraft lignin particles by X-ray scattering. Langmuir 20:9736–9744. https://doi.org/10.1021/la048407v
30. Sieber M, Mehner T, Dietrich D et al (2014) Wear-resistant coatings on aluminium produced by plasma anodising—a correlation of wear properties, microstructure, phase composition and distribution. Surf Coat Technol 240:96–102. https://doi.org/10.1016/j.surfcoat.2013.12.021
31. Ziebell A (2008) Modelling lignin depolymerisation using size exclusion chromatography. Swinburne University of Technology, Hawthorn